1896
doi:10.1017/S143192761101035X
Microsc. Microanal. 17 (Suppl 2), 2011

Atomic Scale Structural and Chemical Quantification of Non-Stoichiometric Defects in Ti and Bi Doped $BiFeO_3$

L.Q. Wang,* B. Schaffer,*,** A.J. Craven,* I. MacLaren,* S. Miao,*** I.M. Reaney***

* School of Physics and Astronomy, University of Glasgow, Glasgow G12 8QQ, UK
** SuperSTEM, STFC Daresbury Laboratories, Keckwick Lane, Warrington WA4 4AD, UK
*** Department of Materials Science and Engineering, University of Sheffield, Sheffield S1 3JD, UK

$BiFeO_3$ has been the subject of intense interest in recent years on account of possible multiferroic properties. Recently, Reaney and co-workers demonstrated that rare-earth doping can induce the formation of antipolar order with similarities to the $PbZrO_3$ structure [1]. This study reports for the first time studies of the atomic structure and chemistry of nanoscale defects in such materials.

$(Bi_{0.85}Nd_{0.15})(Fe_{0.9}Ti_{0.1})O_3$ ceramics were prepared by conventional mixed oxide synthesis [2]. Samples were prepared for microscopy using a conventional method of mechanical polishing followed by ion beam thinning using Ar ions in a Gatan PIPS initially at 4 kV until the sample was close to perforation, followed by finishing at 500 eV to provide a clean, damage-free surface. Carbon coating of the samples was performed to prevent charging. High resolution STEM was performed at 100 kV accelerating voltage using the C_s-corrected Nion UltraSTEM equipped with a Gatan Enfina spectrometer at the SuperSTEM facility, both for high angle annular dark field (HAADF) imaging and for spectrum imaging (SI) from the same sample area on subsequent days. The SI data was post-processed by principal component analysis using the MSA plugins for Digital Micrograph prior to the generation of the elemental maps in order to reduce noise on the maps [3].

Figure 1a shows an HAADF image of a [001] oriented area showing many of the defects of interest; the characteristic feature of these defects is that there are 8 A site columns at the centre, where 9 would be expected for perfect perovskite. Figure 1b was constructed from 50 sequentially recorded fast acquisitions of a 10 nm square box using 5 μs per pixel dwell time to limit image distortion by sample drift; these 50 acquisitions were cross-correlated, drift corrected and summed using the SDSD plugin for Gatan Digital Micrograph [4]. The resultant image has superb signal to noise, without suffering from the drift inherent in long acquisitions. This was analyzed quantitatively to determine the A-site positions in the image and once correction was made for distortions caused by a small discrepancy between the vertical and horizontal magnifications, the A-site atom positions were determined quantitatively, and five similar defects all showed very consistent core structures.

Figure 2 shows elemental maps of one of these defects calculated from spectrum images. These show that the defects are strongly depleted in B site elements, although some Ti-rich columns are often found around the edges. On the other hand, the two central atom columns are very rich in Nd. The other A-site columns (shown strongly in the HAADF image) must therefore be Bi-rich. The oxygen map still shows some oxygen in the defect. Thus these defects must represent coherent rod-shaped precipitates of a Nd-Bi oxide, projecting through the entire thickness of the sample.

Ti donor doping has been used in a related study [2] to control the conductivity of $Bi_{0.85}Nd_{0.15}O_3$ ceramics. < 3 mol% Ti on the B-site has little effect on the structure but above this concentration, the

antipolar order is gradually destroyed according to X-ray diffraction data. The work reported here illustrates how increasing the Ti concentration to > 3 mol% not only destroys antipolar coupling but also modifies the phase assemblage of the ceramic so that Nd rich coherent precipitates are formed. The observations give detailed knowledge of how Ti ions are incorporated into the $Bi_{0.85}Nd_{0.15}FeO_3$ lattice at the expense of Nd ions and give a more subtle appreciation of the solid-solubility limits in this complex system.

References

[1] I. Levin, S. Karimi, V. Provenzano *et al*., *Phys. Rev. B* 81 (2010) 020103.
[2] K. Kalantari, I. Sterianou, S. Karimi, *et al.*, submitted to Advanced Functional Materials, 2011.
[2] M. Bosman, M. Watanabe, D.T.L. Alexander, and V.J. Keast, *Ultramicrosc.* 106 (2006) 1024.
[3] B. Schaffer, W. Grogger, and G. Kothleitner, *Ultramicrosc.* 102 (2004) 27–36.
[4] We are grateful to the EPSRC for financial support, with the provision of a PhD studentship for L.Q. Wang, and the provision of time at SuperSTEM (grant reference EP/I000879/1).

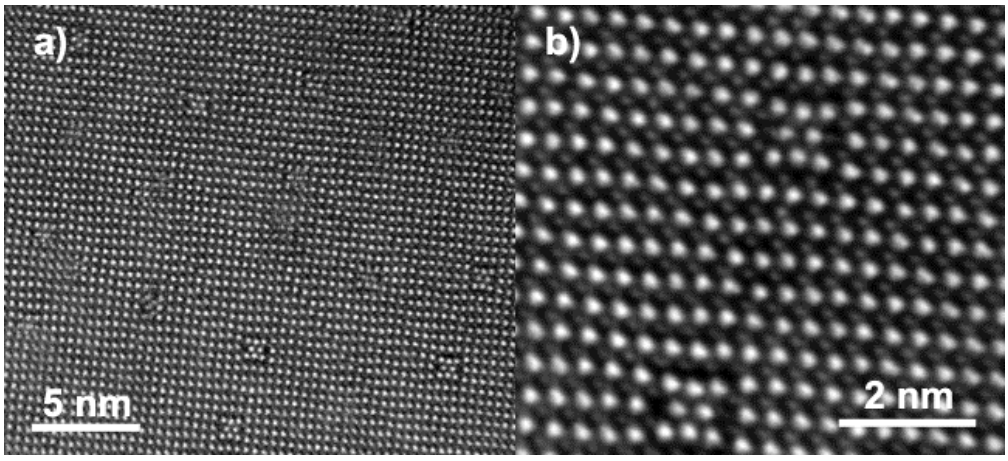

FIG. 1. HAADF images of the defects: a) broader area with many defects; b) image averaged from 50 fast acquisitions

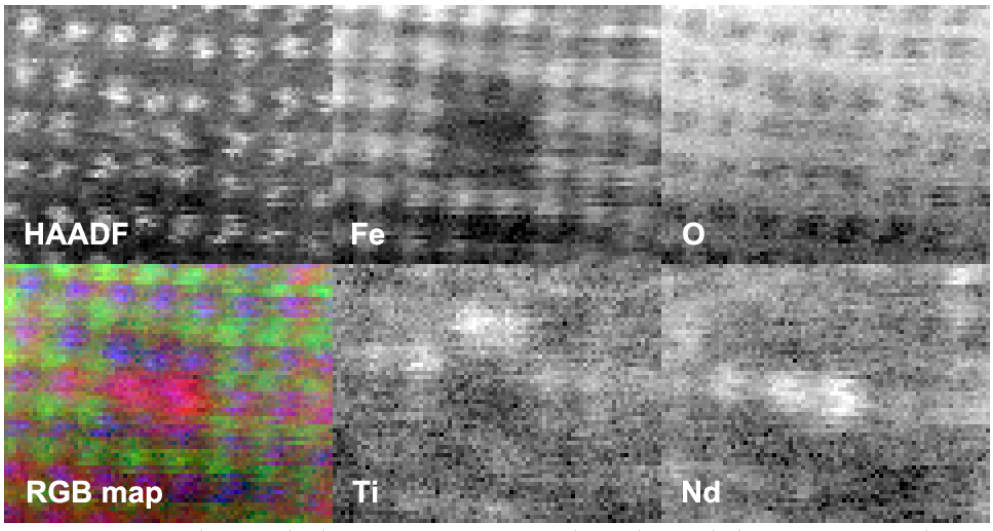

FIG. 2. Atomic resolution EEL spectrum imaging of the structure of one defect. The RGB map created using red for Nd, green for Fe, and blue for HAADF.

https://doi.org/10.1017/S143192761101035X Published online by Cambridge University Press